



HAL
open science

Toward Remote Model-Based Fault Localization in Transmission-Line Networks

Philipp del Hougne

► **To cite this version:**

Philipp del Hougne. Toward Remote Model-Based Fault Localization in Transmission-Line Networks. 2023. hal-04177093

HAL Id: hal-04177093

<https://hal.science/hal-04177093>

Preprint submitted on 3 Aug 2023

HAL is a multi-disciplinary open access archive for the deposit and dissemination of scientific research documents, whether they are published or not. The documents may come from teaching and research institutions in France or abroad, or from public or private research centers.

L'archive ouverte pluridisciplinaire **HAL**, est destinée au dépôt et à la diffusion de documents scientifiques de niveau recherche, publiés ou non, émanant des établissements d'enseignement et de recherche français ou étrangers, des laboratoires publics ou privés.

Toward Remote Model-Based Fault Localization in Transmission-Line Networks

Philipp del Hougne

Univ Rennes, CNRS, IETR-UMR 6164, F-35000 Rennes, France

Correspondence to philipp.del-hougne@univ-rennes1.fr

We analytically derive the updates of a transmission-line network's interaction matrix and scattering matrix as a consequence of a fault (an interrupted transmission line). We find that the fault alters not only the direct coupling between the two nodes that were previously connected by the faulty cable, but that the fault also alters these nodes' self-interactions in a non-trivial manner. Given the network's topology, it is then possible to *remotely* localize the fault on the faulty cable based on measurements of the faulty network's scattering coefficient(s). Our analytical expressions make it possible to efficiently calculate the expected scattering matrix for different fault locations (orders of magnitude faster than a brute-force evaluation). We report a simple demonstration for which we assume to know the network's topology as well as which cable is faulty; we identify the location of the fault on the faulty cable by comparing the broadband scattering coefficient(s) swept across candidate fault locations to the one(s) measured on the faulty network.

Keywords: Transmission-Line Network, Fault Localization, Model-Based Remote Sensing, Physics-Compliant Model, Quantum Graph, Isospectral Reduction

I. INTRODUCTION

In a simple cable, a fault is easily localized via a time-domain analysis of the reflection or transmission coefficient of the cable. In this paper, we are interested in the more challenging problem of localizing a fault in a cable that is part of a complex transmission-line network. We thus cannot probe the cable in isolation nor directly. We can only probe the cable remotely via the asymptotic scattering channels connecting the network to the outside world. In general, the asymptotic scattering channels are not directly connected to the faulty cable of interest.

Our goal of localizing the fault is a problem of sensing in a complex scattering medium. On the one hand, the reverberation in such a complex system can drastically enhance the achievable resolution because it boosts the wave's sensitivity to the perturbation of interest. Indeed, we recently demonstrated a direct link between the resolution with which an object can be localized inside a chaotic cavity and the dwell time of the wave inside the cavity [1]. The chaotic cavity acts essentially like a generalized interferometer, and the resulting interferometric sensitivity can yield orders of magnitude finer resolution than in free space. Deeply sub-wavelength resolution without capturing evanescent waves is thereby feasible [1]. On the other hand, the data analysis inevitably must take into account the specific system's complexity. In Ref. [1], the chaotic cavity's exact geometry and material composition were unknown such that a calibration dataset had to be measured to characterize the specific system's complexity. In contrast, in the present case of a transmission-line network, the topology is usually known, so that its complexity can be taken into account without the need for calibration measurements.

The considered problem of remotely localizing a network fault is of practical importance, for instance, to diagnose line outages in large networks. Currently, such problems are often studied under simplifying assumptions (e.g., using a DC approximation of AC power flow models) and assuming that a line outage simply removes a line from the network topology [2]. Our analytical calculations in the present paper based on a physical model suggest that a fault additionally impacts (in a significant and non-trivial manner) the self-interactions of the nodes that were connected by the faulty line.

Meanwhile, we note that other physics-based remote-sensing approaches for transmission-line networks are currently studied in the literature. For example, Ref. [3] considers the

case of an initial network being split at various edges and nodes into two networks; it is shown in Ref. [3] that by determining the networks' Euler characteristic from scattering measurements [4], one can determine at how many edges and nodes the initial network was split – even without knowing its topology.

In the present paper, we derive an analytical expression for how a fault alters the interaction matrix of a given network, and thereby the observable scattering coefficient(s). We numerically validate the derived expressions and demonstrate their application to remote model-based fault localization.

II. GENERALITIES

In this section, we recall the well-established background on wave scattering in a transmission-line network on which our subsequent analysis builds.

A transmission-line network, also known as “quantum graph” [5–7], can be understood as being composed of non-resonant scattering entities (its nodes, i.e., the junctions) that have certain couplings between each other (its bonds, i.e., the cables) and with the outside world (the asymptotic scattering channels). Let us consider a system composed of n nodes of which $m \leq n$ are directly connected to an asymptotic scattering channel; we assume that each asymptotic scattering channel is non-dispersively coupled to exactly one node.

The considered transmission-line networks are also known as Neumann quantum graphs, and Refs. [6, 8, 9] derived an exact expression relating the system's scattering matrix $\mathbf{S} \in \mathbb{C}^{m \times m}$ to the network topology:

$$\mathbf{S} = \mathbf{I}_m - 2i\mathbf{W}^\dagger \frac{1}{\mathbf{H} + i\mathbf{W}\mathbf{W}^\dagger} \mathbf{W}. \quad (1)$$

The matrices involved in Eq. (1) are defined as follows:

1. $\mathbf{I}_m \in \mathbb{B}^{m \times m}$ is an identity matrix.
2. $\mathbf{W} \in \mathbb{B}^{n \times m}$ is the coupling matrix describing the coupling between each node and each asymptotic scattering channel. If the i th meta-atom is connected to the j th asymptotic scattering channel, the (i, j) th entry of \mathbf{W} is unity; otherwise, it is zero.
3. $\mathbf{H} \in \mathbb{R}^{n \times n}$ is the interaction matrix of the transmission-line network. Its (i, j) th entry

is defined as follows:

$$H_{i,j} = \begin{cases} -\sum_{l \neq i} C_{i,l} \cot(kL_{i,l}) & \text{if } i = j. \\ C_{i,j} \csc(kL_{i,j}) & \text{otherwise.} \end{cases} \quad (2)$$

Here, $C_{i,j}$ is unity if the nodes indexed i and j are directly connected, and zero otherwise. $L_{i,j}$ is the length of the cable connecting the nodes indexed i and j . k is the wavenumber. We limit ourselves to reciprocal bonds in the present paper, so \mathbf{H} is a symmetric matrix. Moreover, its dependence on the wavenumber implies that \mathbf{H} , and therefore also \mathbf{S} , are frequency-dependent.

III. PHYSICS-COMPLIANT FAULT MODEL

The fault considered in this paper is illustrated in Fig. 1: the cable of length L linking nodes α and β is cut at a distance L_1 from α . This fault implies that the direct link between nodes α and β is interrupted, but this fault is *not* equivalent to just removing the cable between α and β . Waves will still travel along the faulty cable and will be reflected by the

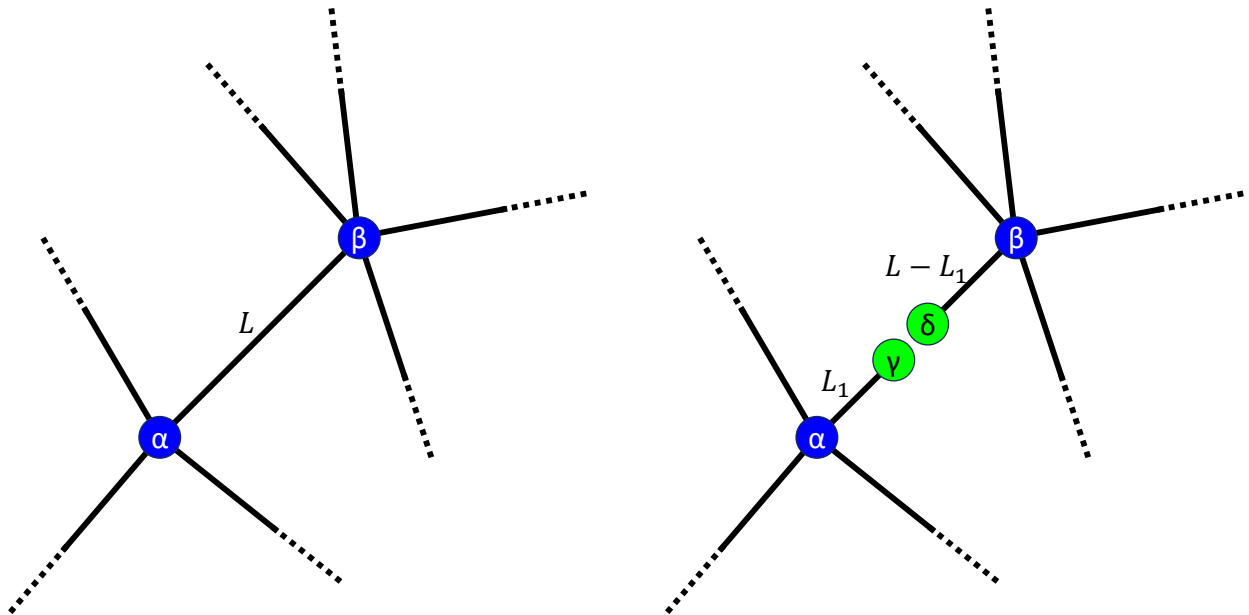


FIG. 1. Considered fault: the cable linking nodes α and β is interrupted (cut) at a distance L_1 from α , creating two new nodes γ and δ . The sketches on the left and right show, respectively, the intact and faulty cable of interest within a larger transmission-line network.

fault, which we assume to be an open-circuit end. Therefore, the physics-compliant fault model consists of two modifications of the original network topology:

1. Removal of the cable linking α and β .
2. Creation of two new nodes, γ and δ , which are directly connected to α and β via cables of length L_1 and $L - L_1$, respectively.

Let us denote by \mathbf{H}_0 and \mathbf{S}_0 the interaction matrix and scattering matrix, respectively, of the intact transmission-line network of interest. Assuming the network topology is known, \mathbf{H}_0 and \mathbf{S}_0 are also known analytically. After the appearance of the fault, the faulty network is described by \mathbf{H}_1 and \mathbf{S}_1 . Note that the dimensions of \mathbf{H}_1 are $(n + 2) \times (n + 2)$ because of the two new nodes γ and δ .

We assume to know (i) the network topology, and (ii) which cable is faulty, and we seek to localize the fault on the faulty cable by estimating L_1 . Our next goal is hence to now find an analytical expression for $\Delta\mathbf{S} = \mathbf{S}_1 - \mathbf{S}_0$ as a function of the sought-after parameter L_1 .

IV. INTERACTION MATRIX UPDATE DUE TO FAULT

As a first step, we seek to identify in this section how the interaction matrix of our network must be updated to account for the fault. Without loss of generality, we index the nodes of the intact network such that α and β have indices $(n - 1)$ and n , respectively.

So far, we have considered the interaction matrix always in the canonical basis, where its dimensions directly correspond to the number of nodes. However, there are equivalent representations reduced to a subset of the nodes. Indeed, the nodes that are not directly connected to asymptotic scattering channels can equivalently be understood as merely being a non-local coupling mechanism between the remaining nodes. Mathematically, such a reduced-basis representation is based on the block matrix inversion lemma. Calculations of reduced-basis interaction matrixes were presented in contexts ranging from tight-binding network engineering [10] to isospectral graph reduction [11]. In particular, recently we used them to achieve covert symmetry-based wave scattering control by covertly encoding the symmetry in non-local interactions between “primary” meta-atoms such that the symmetry is “hidden”, i.e., the symmetry is only apparent in a reduced basis but not in the canonical

$$\mathbf{H}_1^{\text{red}} = \mathbf{H}_0 + \underbrace{\Delta}_{\substack{\dots \\ \vdots \\ \alpha \quad \beta \\ \vdots \\ \alpha \quad \beta \\ a \quad b \\ b \quad c}} - \underbrace{\mathbf{X}}_{\substack{\gamma \quad \delta \\ \alpha \\ \beta}} \underbrace{\mathbf{Z}^{-1}}_{\left(\begin{array}{cc} \alpha & \gamma \quad \delta \\ \beta & \quad \quad \end{array} \right)^{-1}} \underbrace{\mathbf{Y}}_{\substack{\alpha \quad \beta \\ \gamma \quad \delta \\ a \quad b \\ b \quad c \\ e}} = \mathbf{H}_0 + \underbrace{\Gamma}_{\substack{\dots \\ \vdots \\ \alpha \quad \beta \\ \vdots \\ \alpha \quad \beta \\ p \quad b \\ b \quad q}}$$

$$\begin{aligned} a &= \cot(kL) - \cot(kL_1) \\ b &= -\csc(kL) \\ c &= \cot(kL) - \cot(k(L-L_1)) \\ d &= \csc(kL_1) \\ e &= \csc(k(L-L_1)) \\ f &= -\cot(kL_1) \\ g &= -\cot(k(L-L_1)) \\ p &= a - d^2/f \\ q &= c - e^2/g \end{aligned}$$

FIG. 2. Fault-induced update of the interaction matrix in the reduced $n \times n$ basis. The update concerns the 2×2 block of the interaction matrix involving nodes α and β .

basis [12]; very recently, we also used a reduced-basis representation to formulate and calibrate compact physics-compliant models of massively parametrized complex media such as “smart” radio environments [13, 14].

In the present context, the two fault-induced new nodes γ and δ are certainly not directly connected to any asymptotic scattering channel (they have only one connection to α or β , respectively). Therefore, we can find an equivalent representation of \mathbf{H}_1 in the basis reduced to the n initial nodes. We begin by writing \mathbf{H}_1 in block form:

$$\mathbf{H}_1 = \begin{bmatrix} \mathbf{H}_{1,n} & \mathbf{X} \\ \mathbf{Y} & \mathbf{Z} \end{bmatrix}, \quad (3)$$

where $\mathbf{H}_{1,n} \in \mathbb{R}^{n \times n}$, $\mathbf{X} \in \mathbb{R}^{n \times 2}$, $\mathbf{Y} \in \mathbb{R}^{2 \times n}$, and $\mathbf{Z} \in \mathbb{C}^{2 \times 2}$. Then, the reduced-basis representation of \mathbf{H}_1 is

$$\mathbf{H}_1^{\text{red}} = \mathbf{H}_{1,n} - \mathbf{X}\mathbf{Z}^{-1}\mathbf{Y}. \quad (4)$$

Since our goal is to express $\mathbf{H}_1^{\text{red}}$ as an update of \mathbf{H}_0 , we introduce $\Delta = \mathbf{H}_{1,n} - \mathbf{H}_0$. Now, we can formulate the impact of the fault as an update of the original interaction matrix:

$$\mathbf{H}_1^{\text{red}} = \mathbf{H}_0 + \Delta - \mathbf{X}\mathbf{Z}^{-1}\mathbf{Y} = \mathbf{H}_0 + \Gamma. \quad (5)$$

Next, we seek to define the entries of $\Gamma = \Delta - \mathbf{X}\mathbf{Z}^{-1}\mathbf{Y}$ in terms of L_1 . This procedure is illustrated in Fig. 2. The only non-zero entries of Δ are the ones in its bottom right 2×2 block:

$$\Delta_{n-1,n-1} = a = \cot(kL) - \cot(kL_1). \quad (6a)$$

$$\Delta_{n-1,n} = \Delta_{n,n-1} = b = -\csc(kL) \quad (6b)$$

$$\Delta_{n,n} = c = \cot(kL) - \cot(k(L - L_1)) \quad (6c)$$

The only non-zero entries of $\mathbf{X} = \mathbf{Y}^T$ are the following two:

$$X_{n-1,1} = Y_{1,n-1} = d = \csc(kL_1). \quad (7a)$$

$$X_{n,2} = Y_{2,n} = e = \csc(k(L - L_1)). \quad (7b)$$

The entries of \mathbf{Z} are as follows:

$$Z_{1,1} = f = -\cot(kL_1). \quad (8a)$$

$$Z_{1,2} = Z_{2,1} = 0. \quad (8b)$$

$$Z_{2,2} = g = -\cot(k(L - L_1)). \quad (8c)$$

Ultimately, we find that only the bottom right 2×2 block of $\mathbf{\Gamma}$ is non-zero:

$$\Gamma_{n-1,n-1} = p = a - \frac{d^2}{f} = \cot(kL) - \cot(kL_1) + \frac{(\csc(kL_1))^2}{\cot(kL_1)}. \quad (9a)$$

$$\Gamma_{n-1,n} = \Gamma_{n,n-1} = b = -\csc(kL). \quad (9b)$$

$$\Gamma_{n,n} = q = c - \frac{e^2}{g} = \cot(kL) - \cot(k(L - L_1)) + \frac{(\csc(k(L - L_1)))^2}{\cot(k(L - L_1))}. \quad (9c)$$

Therefore, the fault has not only removed the direct coupling between α and β , but it has also changed the self-interactions of α and β in a non-trivial way. One possible interpretation is that in the reduced basis, α and β are now resonant because they have a cable of length L_1 or $L - L_1$, respectively, with open-circuit termination attached to them.

V. SCATTERING MATRIX UPDATE DUE TO FAULT

In the previous section, we expressed the impact of the fault as an update (parametrized by L_1) of the interaction matrix. In this section, we now evaluate how the scattering matrix of the network is updated due to the fault. As seen in Eq. (1), to go from the interaction matrix \mathbf{H} to the scattering matrix \mathbf{S} , the matrix $\mathbf{G} = \mathbf{H} + i\mathbf{W}\mathbf{W}^\dagger$ must be inverted. We define

$$\mathbf{G}_1 = \mathbf{H}_1^{\text{red}} + i\mathbf{W}\mathbf{W}^\dagger = \mathbf{H}_0 + \mathbf{\Gamma} + i\mathbf{W}\mathbf{W}^\dagger = \mathbf{G}_0 + \mathbf{\Gamma} = \mathbf{G}_0 + \mathbf{U}\mathbf{D}\mathbf{V}, \quad (10)$$

where

$$\mathbf{U} = \begin{bmatrix} \mathbf{0}_{n-2,2} \\ \mathbf{Q} \end{bmatrix} \quad \text{and} \quad \mathbf{V} = \begin{bmatrix} \mathbf{0}_{n-2,2}^T & \mathbf{Q}^{-1} \end{bmatrix}, \quad (11)$$

\mathbf{QDQ}^{-1} is the eigendecomposition of the bottom right 2×2 block of $\mathbf{\Gamma}$, and $\mathbf{0}_{n-2,2}$ is a $(n-2) \times 2$ matrix of zeros.

Based on the Woodbury matrix identity, we obtain

$$\mathbf{G}_1^{-1} = \mathbf{G}_0^{-1} - \mathbf{G}_0^{-1}\mathbf{U}(\mathbf{D}^{-1} + \mathbf{V}\mathbf{G}_0^{-1}\mathbf{U})^{-1}\mathbf{V}\mathbf{G}_0^{-1} \quad (12)$$

and hence

$$\mathbf{S}_1 = \mathbf{I} - 2i\mathbf{W}^\dagger\mathbf{G}_1^{-1}\mathbf{W} = \mathbf{S}_0 + 2i\mathbf{W}^\dagger(\mathbf{G}_0^{-1}\mathbf{U}(\mathbf{D}^{-1} + \mathbf{V}\mathbf{G}_0^{-1}\mathbf{U})^{-1}\mathbf{V}\mathbf{G}_0^{-1})\mathbf{W}. \quad (13)$$

Next, we seek to express \mathbf{Q} and \mathbf{D} in terms of L_1 so that we can analytically relate the change of the observable scattering coefficient(s) to L_1 . An analytical eigendecomposition of the bottom right 2×2 block of $\mathbf{\Gamma}$ yields

$$\mathbf{Q} = \begin{bmatrix} \frac{-(q-p+z)}{2b} & \frac{p-q+z}{2b} \\ 1 & 1 \end{bmatrix}, \quad (14a)$$

$$\mathbf{D} = \text{diag} \left(\left[\frac{p+q-z}{2} \quad \frac{p+q+z}{2} \right] \right), \quad (14b)$$

where $z = \sqrt{p^2 - 2pq + q^2 + 4b^2}$, and the diag operator constructs a diagonal matrix from a vector.

Equations (13) and (14) are the key result of the present paper, analytically relating the update of \mathbf{S} due to the fault to L_1 .

VI. APPLICATION TO AN EXAMPLE NETWORK

In this section, we consider a specific example network (i) to validate the key result of our analytical calculations [i.e., Eq. (13)], and (ii) to demonstrate its use for fault localization.

A. Numerical Validation of Eq. (13)

We consider the example random transmission-line network shown in Fig. 5. Two asymptotic scattering channels are connected to the network, and one of the network's inner cables is interrupted by a fault. We assume a wave speed of 70 % of the speed of light in free space.

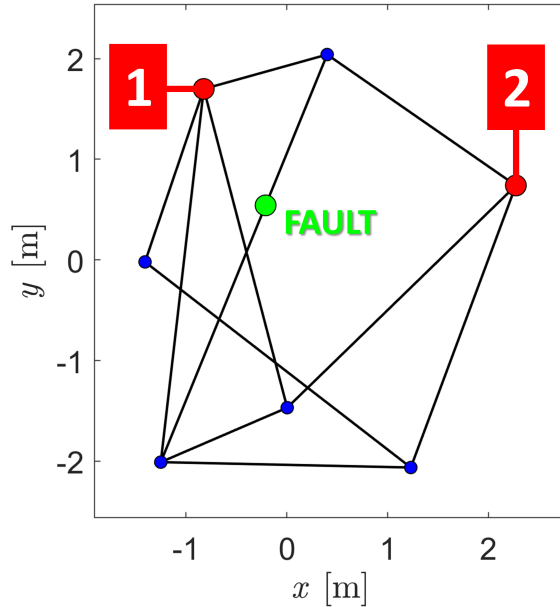


FIG. 3. The considered random transmission-line network. Each of the two red nodes is directly connected to one asymptotic scattering channel. The location of the fault, at which the faulty cable is interrupted, is highlighted in green.

We plot in Fig. 4 the frequency-dependent scattering coefficients of the intact (blue) and faulty (red) networks. The fault has very significantly altered the network’s scattering matrix. The blue and red curves are evaluated with the brute-force approach from Eq. (2). However, in the case of the faulty network, the scattering coefficients can be more efficiently evaluated as updates of the intact network’s scattering coefficients with Eq. (13), yielding the yellow lines in Fig. 4. The agreement between red and yellow lines validates the analytical expression from Eq. (13).

B. Remote Model-Based Fault Localization

The faulty network’s transmission coefficient $S_{21}(f)$ is a wave fingerprint of the fault’s location [1, 15, 16]. Given Eq. (13), we can now analytically calculate the expected transmission spectra for different candidate fault locations L_1 , in order to identify the one that best explains the measured $S_{21}(f)$ of the faulty network.

For the sake of simplicity, we assume negligible measurement noise. For our analysis, we restrict ourselves to a rather small (arbitrarily chosen) frequency interval, $37.3 \text{ MHz} <$

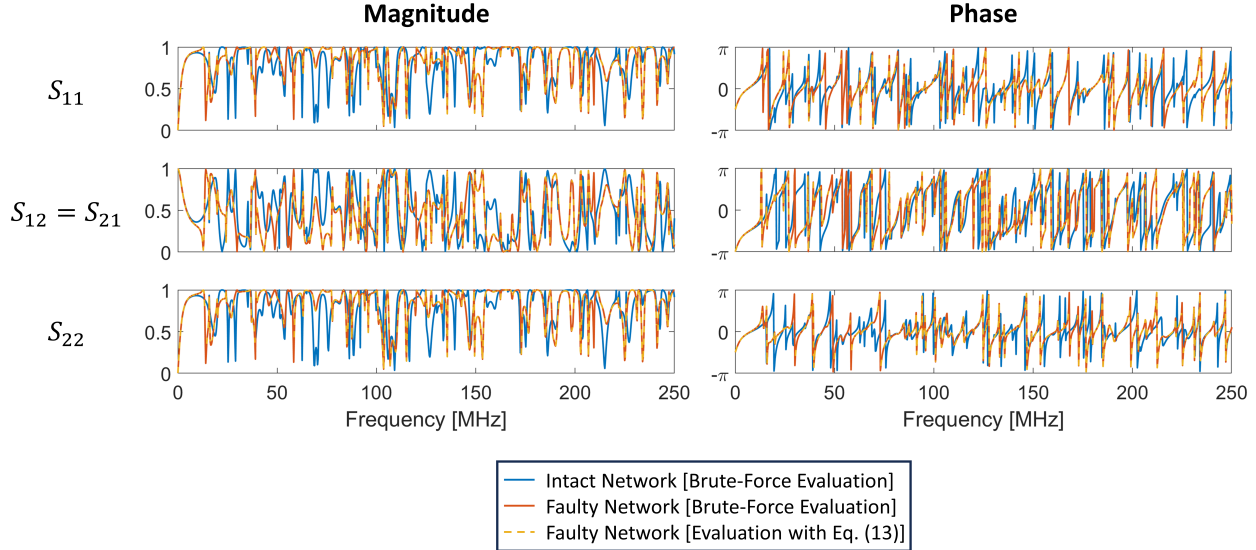


FIG. 4. Comparison of the frequency-dependent scattering coefficients in terms of magnitude (right) and phase (left) for the intact network (blue), the faulty network (red), and the faulty network evaluated with Eq. (13) (yellow).

$f < 49.8$ MHz, with 50 linearly spaced frequency points. We consider 1000 linearly spaced candidate values of L_1 between zero and the length of the cable connecting α and β in the intact network. For each candidate value of L_1 , we compute the correlation coefficient of the transmission spectrum with that measured on the faulty network. Our estimate of L_1 is then simply the candidate value with the highest correlation coefficient. Our results displayed in Fig. 5 provide an accurate estimate of L_1 , orders of magnitude better than the smallest measured wavelength (4.2 m for 49.8 MHz).

Of course, the data analysis method can be refined to endow it with robustness against measurement noise [1] and/or environmental perturbations [16], for example by training an artificial neural network for the wave fingerprint identification, as reported in Refs. [1, 16] for localization in a chaotic cavity. Applying these techniques to the localization of faults in transmission-line networks is left for future work. The main purpose of the present work is to demonstrate that in the case of a transmission-line network, wave-fingerprint based localization techniques can be applied using an efficient physics-compliant model instead of having to collect experimental calibration data.

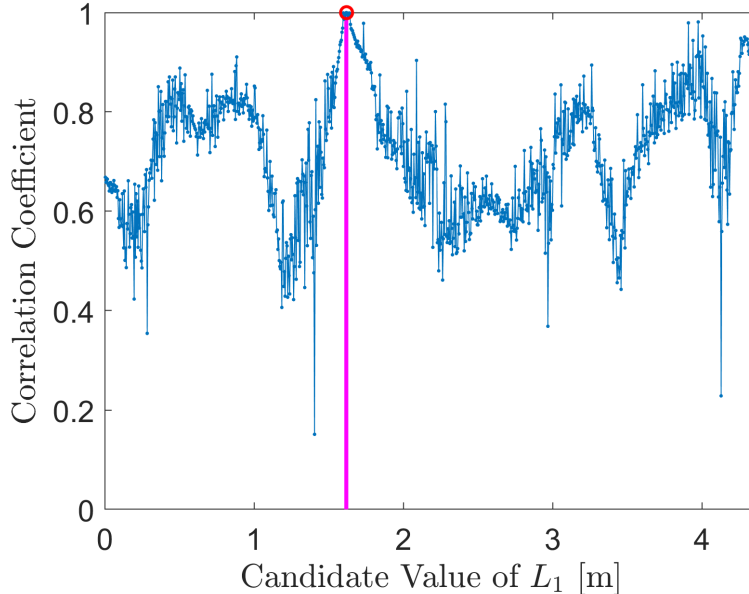


FIG. 5. Demonstration of remote model-based fault localization for the faulty network from Fig. 5. The vertical magenta-colored line indicates the ground-truth value of L_1 .

VII. CONCLUSION

To summarize, we have derived an analytical expression for the update of a transmission-line network's scattering matrix due to a fault. We found that, besides removing the direct connection between two nodes, a fault also significantly alters the self-interactions of these two nodes in a rather complicated manner. Using the derived physics-compliant model, we *remotely* localized a fault in an example random network with high accuracy based on the faulty network's transmission spectrum. Looking forward, the signal-processing aspects of the methodology can be refined to remove the need for knowing which cable is the faulty one, and to be resilient against noise and environmental perturbations. Naturally, experimental validations at various scales are also envisioned.

-
- [1] M. del Hougne, S. Gigan, and P. del Hougne, Deeply subwavelength localization with reverberation-coded aperture, *Phys. Rev. Lett.* **127**, 043903 (2021).
 - [2] Y. Zhao, J. Chen, and H. V. Poor, A learning-to-infer method for real-time power grid multi-line outage identification, *IEEE Trans. Smart Grid.* **11**, 555 (2019).

- [3] O. Farooq, A. Akhshani, M. Białous, S. Bauch, M. Ławniczak, and L. Sirko, Investigation of the generalized euler characteristic of graphs and microwave networks split at edges and vertices, *Phys. Scr.* **98**, 024005 (2023).
- [4] M. Ławniczak, P. Kurasov, S. Bauch, M. Białous, V. Yunko, and L. Sirko, Hearing euler characteristic of graphs, *Phys. Rev. E* **101**, 052320 (2020).
- [5] T. Kottos and U. Smilansky, Quantum chaos on graphs, *Phys. Rev. Lett.* **79**, 4794 (1997).
- [6] T. Kottos and U. Smilansky, Quantum graphs: a simple model for chaotic scattering, *J. Phys. A* **36**, 3501 (2003).
- [7] O. Hul, S. Bauch, P. Pakoński, N. Savytskyy, K. Życzkowski, and L. Sirko, Experimental simulation of quantum graphs by microwave networks, *Phys. Rev. E* **69**, 056205 (2004).
- [8] C. Texier and G. Montambaux, Scattering theory on graphs, *J. Phys. A* **34**, 10307 (2001).
- [9] P. Kuchment, Quantum graphs: I. Some basic structures, *Waves Random Media* **14**, S107 (2003).
- [10] S. Longhi, Non-Hermitian tight-binding network engineering, *Phys. Rev. A* **93**, 022102 (2016).
- [11] L. Bunimovich and B. Webb, Isospectral transformations, *Springer Monogr. Math.* (2014).
- [12] J. Sol, M. Röntgen, and P. del Hougne, Covert scattering control in metamaterials with non-locally encoded hidden symmetry, *arXiv:2305.00906* (2023).
- [13] H. Prod'homme and P. del Hougne, Efficient computation of physics-compliant channel realizations for (rich-scattering) RIS-parametrized radio environments, *arXiv:2306.00244* (2023).
- [14] J. Sol, H. Prod'homme, L. Le Magoarou, and P. del Hougne, Experimentally realized physical-model-based wave control in metasurface-programmable complex media, *hal-04174477* (2023).
- [15] P. del Hougne, M. F. Imani, M. Fink, D. R. Smith, and G. Lerosey, Precise localization of multiple noncooperative objects in a disordered cavity by wave front shaping, *Phys. Rev. Lett.* **121**, 063901 (2018).
- [16] P. del Hougne, Robust position sensing with wave fingerprints in dynamic complex propagation environments, *Phys. Rev. Research* **2**, 043224 (2020).